Calcium Concentration and Movement in the Diadic Cleft Space of the Cardiac Ventricular Cell

G. A. Langer*‡ and A. Peskoff‡§
Cardiovascular Res. Laboratory and the Departments of *Medicine, ‡Physiology, and §Biomathematics, UCLA School of Medicine, Los Angeles, California 90095-1760 USA

ABSTRACT We model the space between the junctional sarcoplasmic reticulum (JSR) membrane and the inner leaflet of the transverse tubular ("T") sarcolemmal (SL) membrane, the diadic cleft, with respect to calcium (Ca) concentration and movement. The model predicts the following: 1) Ca influx via the "L" channel increases [Ca] to 1 μM within a distance of 50 nm from the channel mouth in <500 μs. This is sufficient to trigger Ca release from a domain of 9 "feet." 2) By contrast, "reverse" Na/Ca exchange will increase [Ca] to ~0.5 μM throughout the cleft space in 10 ms, sufficient to trigger Ca release, but clearly to a lesser extent and more slowly than the channel. 3) After a 20-ms JSR release into the cleft via the "feet" [Ca] peaks at 600 μM (cleft center) to 100 μM (cleft periphery) and then declines to diastolic level (100 nM) within 150 ms throughout the cleft. 4) The ratio of flux out of the cleft via Na/Ca exchange to flux out of the cleft to the cytosol varies inversely as JSR Ca release. 5) Removal of SL anionic Ca-binding sites from the model will cause [Ca] to fall to 100 nM throughout the cleft in <1 ms after JSR release ceases. This markedly reduces Na/Ca exchange. 6) Removal from or decreased concentration of Na/Ca exchangers in the cleft will cause [Ca] to fall too slowly after JSR release to permit triggered release upon subsequent excitation.

INTRODUCTION

A number of studies over the past 20 years have proposed and/or provided evidence for subcellular "restricted spaces" (Bassingthwaighte and Reuter, 1972; Leblanc and Hume, 1990; Lederer et al., 1990; Carmeliet, 1992; Moore et al., 1993; Niggli and Lipp, 1993; Kargacin, 1994), particularly with respect to Na and Ca, in various types of muscle. A "restricted space" of particular interest is the space between the lateral cistern of the sarcoplasmic reticulum (SR) and the inner sarcolemmal (SL) membrane in cardiac cells. This has been termed the "fuzzy space" (Lederer et al., 1990) but has rather well-defined characteristics. It is the region that contains the "feet" (Inui et al., 1987) from which, it is now generally accepted, Ca is released from the SR (Ikemoto et al., 1991; Jorgensen et al., 1993). We have designated this space the "diadic cleft" and have presented an initial model for Ca concentration and diffusion in the cleft after its release from the feet into the cleft space (Peskoff et al., 1992).

It was expected that, given the small volume of the space and moderately restricted diffusion, that release of cisternal Ca would produce a manyfold increase in [Ca] in the space, which would then fall rapidly upon cessation of the 20-ms release. Release of an amount of Ca sufficient to produce maximum contractile force (2.8×10^{-15} mol/cell) (Fabiato, 1983) caused [Ca] to rise to a level of ~1 mM in the cleft during release but then to fall by four orders of magnitude to 10^{-7} M within 4 ms after cessation of release (diffusion coefficient 20% of free aqueous diffusion of 5×10^{-6} cm^2/s in the cleft space). Previous experimental work indicated, however, that the model was incomplete. It had been shown that the inner leaflet of the SL contained all of the membrane anionic phospholipid (phosphatidylserine (PS) and phosphatidylinositol (PI)) and 75% of the membrane's zwitterionic phosphatidylethanolamine (PE) (Post et al., 1988). These phospholipids have a low affinity for Ca (K_d = 1.1 mM) but are abundant (900 μmol/liter cell water) (Post and Langer, 1992). Addition of the phospholipid binding sites at the inner SL leaflet to the model in the given amount, and with the K_d as measured, produced a striking change in the cleft's Ca concentration profile (Peskoff et al., 1992).

With the inner leaflet anionic Ca binding sites present [Ca] rose somewhat less during release (~600 μM) but remained above 10 μM for 200 ms after cessation of release. This initial model considered only SR release, Ca binding, and diffusion parameters and did not include an operative Na/Ca exchange system. There is now convincing evidence that Na/Ca exchangers are localized in the diadic areas (Frank et al., 1992). If this is the case, the maintenance of high [Ca] in the diadic clefts would optimize Ca efflux, after its release, via Na/Ca exchange. Recent evidence indicates that the K_d (Ca) of the Na/Ca exchanger is ~5 μM in vivo (Hilgemann et al., 1992). Because [Ca] in the general cytoplasm rarely rises above 1.5 μM, and then for only a few milliseconds (Berlin and Konishi, 1993), optimum operation of the exchanger seems to require that it be located at a specialized, compartmentalized region of the cell. The clefts would qualify as such a region.

Received for publication 19 May 1995 and in final form 13 November 1995.

Address reprint requests to Dr. Glenn A. Langer, Cardiovascular Research Laboratory, UCLA School of Medicine, 675 Circle Drive South, Los Angeles, CA 90095. Tel.: 310-825-6824; Fax: 310-206-5777; E-mail: glenn@cvrl.ucla.edu.

0006-3495/96/03/1169/14 $2.00

The present study updates the cleft model and expands it to include 1) consideration of the [Ca] in the cleft during the period after the start of the action potential but before release of the SR Ca (i.e., the SR Ca trigger stage); 2) the [Na] profile for Na entry into the clefts via the Na channel; 3) [Ca] in the cleft as a result of changes in cleft [Na] and membrane potential and their effect on net movement of Ca via Na/Ca exchange; 4) [Ca] in the cleft space, as a function of time, after junctional sarcoplasmic reticulum (JSR) release; 5) consideration of the proportion of Ca transported out of the cell from the cleft space via Na/Ca exchange as compared to Ca diffusing out of the cleft to the myofilaments as a function of the amount of Ca released.

The results obtained will then be discussed, with focus on 1) determining the most likely Ca-triggering process (Ca flux into the cleft via the Ca channels or via "reverse" Na/Ca exchange?); 2) comparison of "force versus pCa trigger" relation with the predicted cleft [Ca] from the model; 3) efflux via Na/Ca exchange with exchangers localized to the cleft.

THE MODEL

Fig. 1 is a schematic representation of the diadic cleft space with pertinent characteristics listed. The morphometric data of Stewart and Page (1978) and Page (1978) for rats of intermediate weight are used. The cell and sarcomeres are assumed to be right circular cylinders. A cell volume of 1.57×10^4 μm^3 and individual sarcomeric volume of 1.37 μm^3 are derived. Sixty percent of cell volume is assumed to be sarcomeric (Legato, 1979), and therefore there are 6.88×10^3 sarcomeres/cell ($1.57 \times 10^4/1.37 \times 0.6$).

Page (1978) has measured the rat's junctional (cleft) area per total T tube area at 46%. We estimate from examination of various electron micrographs (Frank, 1990) that a radius of 0.2 μm for an assumed circular JSR junction is reasonable, which gives a value of 0.13 μm^2 for a single junction. If there is one junction per sarcomere (a junction per two half-sarcomeres at Z-line level) then the total cleft or junctional area per cell is 894 μm^2 ($6.88 \times 10^3 \times 0.13$). Stewart and Page (1978) measure the transverse tubular area at 1.88×10^3 μm^2 per cell. Therefore, a cleft radius of 0.2 μm with a junction per sarcomere gives a cleft area/T tube area ratio of 48%, essentially the value measured by Page (1978).

The width of the cleft space is assumed to be equal to the height of the feet structures. The dimensions of the feet have been recently measured with cryoelectron microscopy and three-dimensional reconstruction found to be $29 \times 29 \times 12$ nm (Radermacher et al., 1994). With a cleft radius of 0.2 μm and height of 12 nm the volume of an individual cleft space (Fig. 1) is 1.5×10^{-3} μm^3. The actual cleft is, of course, not circular. Its shape is not known but is likely to be irregular. The two circular areas (SR and SL) in the model, rather than being flat, are actually wrapped around a T tubule. Because the ratio of radius to width (200/12 = 16.7) is large, the assumption of flatness will have an insignificant effect on the calculated Ca diffusion.

Wibo et al. (1991) found a concentration of L-type Ca^{2+} channels in the diadic junctions of rat ventricle in close association with the ryanodine receptors (feet) of the SR. Ca channels were at a density of 84/μm^2 junctional area and the feet at a density of 765/μm^2 in the junction. Given the junctional area of 0.13 μm^2, this would place 11 Ca channels and 100 feet within each junction—a ratio of 1:9. Fig. 2 represents our proposed relation for the domain of a single Ca channel placed in the center of an array of nine feet. Each of the feet has a volume of 1×10^{-5} μm^3, and if there are 100 within an individual cleft then 67% of the cleft volume is occupied by feet structures.

Hilgemann et al. (1991) estimated that guinea pig cardiac sarcolemma had about 400 Na/Ca exchangers/μm^2 distributed over the surface of the cell. In their immunofluorescence study using monoclonal antibody to the Na/Ca exchanger, Frank et al. (1992) show a clear increase in concentration of the exchangers in the T tubes as compared to the cell surface. There is, however, no quantitative estimate as to the magnitude of the increase. For the sake of present modeling and until quantitation is available we double the Na/Ca exchanger concentration in the cleft sarcolemma, i.e., 800 exchangers/μm^2.

The model includes the presence of anionic Ca-binding sites on the inner sarcolemmal leaflet (Fig. 1). Two classes of binding sites have been found and characterized in rat neonatal cultured cells (Post and Langer, 1992): 1) K_d = 1.1 mM, capacity 84 nmol/mg; 2) K_d = 13 μM, capacity 7 nmol/mg SL protein. It has been determined that the predominant low-affinity sites are the Ca-binding inner-leaflet phospholipids, phosphatidyserine, -inositol, and -ethanolamine (Post and Langer, 1992). These sites are a major factor in the determination of Ca concentration and movement within the cleft space. The affinity of Na for these sites is derived from the study by Ohki and Kurland (1981) on divalent and monovalent ion binding to phosphatidylserine monolayers. Na binds with an affinity 2% that of Ca or a K_d = 55 mM for the low-affinity sites. Although we have no experimental evidence for such, we assume that the affinity for the high-affinity sites is proportional.

We model the "L" channel for Ca and the Na channel as entering directly into the cleft space. The Ca channel current is assumed to be a 1-ms rectangular pulse with a peak of 0.3 pA (Rose et al., 1992) and the Na channel current a trapezoidal pulse (500 μs zero to peak, 500 μs at peak, 500 μs peak to zero) with a peak of 2 pA (Böhle and Benndorf, 1995). A model for Ca entering or leaving a semi-infinite region via a Ca channel was given by Bers and Peskoff (1991).

The diffusion coefficient, D, is assumed to be 1×10^{-6} cm^2/s for Ca within the cleft space, and 2×10^{-6} cm^2/s for Na. This is an estimate based on the measured free diffusion in aqueous solution of $5–7 \times 10^{-6}$ cm^2/s for Ca (Wang, 1953; Hodgkin and Keynes, 1957; Kushmerick and Podolsky, 1969; Nasi and Tillotson, 1985) and 1.34×10^{-5} cm^2/s for Na (Bockris and Reddy, 1970), and an approximation to account for the presence of the array of rectangular feet

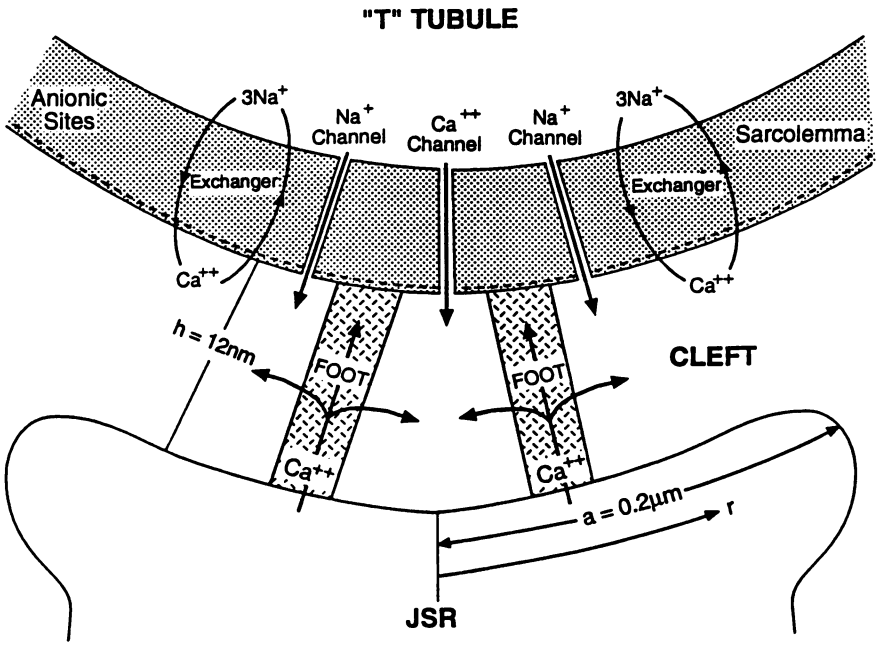

FIGURE 1 Schematic representation of the cardiac diadic cleft space. Pertinent characteristics used in the model are summarized below. See Model for details. Schematic is not to scale.

CLEFT CHARACTERISTICS

Radius - 0.2μm
Height - 12 nm
Junctional Area - 0.13 μm^2
Junctional Volume - 1.5 $x10^{-3}$ μm^3
Cleft Area/T tube area - 0.48
Cleft Density - 1/sarcomere
Feet/Ca channel - 9/1
"Feet" Vol/Cleft Vol.-0.67
Na/Ca Exchanger Density - 800/μm^2
Anionic SL inner leaflet sites
Ca low affinity (K_d = 1.1 mM) - 2.3 x 10^{-19} mols/cleft
Ca high affinity (K_d = 13 μm) - 1.9 x 10^{-20} mols/cleft
Na affinity for sites - K_d ~ 55 mM
Ca current - 0.3 pA peak (1 msec ramp)
Na current - 2 pA peak (trapezoidal pulse)
Ca flux into cleft from SR 2.0 x 10^{-19} mols/beat

Diffusion in cleft space
D = 1.0 x 10^{-6} cm^2/sec (Ca)
D = 2.0 x 10^{-6} cm^2/sec (Na)

within the cleft (Fig. 2). Crank (1975) discusses diffusion problems in a two-phase heterogeneous medium and shows that diffusion through such a system of barriers can be approximated by diffusion in the same region without barriers but with a reduced effective diffusion coefficient. The free diffusion coefficient is multiplied by a "window" factor which, for diffusion through one of the passages between two feet, is 7 nm/36 nm = 0.19. The spreading of the lines of flow as ions diffuse through the intersection between two orthogonal passages yields a slightly higher effective value. The presence of other obstacles, besides the feet, would further reduce the effective diffusion coefficient. Our assumption of 1 and 2 $\times$ 10^{-6} cm^2/s for Ca and Na, respectively, is therefore probably a conservative reduction from free diffusion.

The value chosen for Ca flux into the cleft from the JSR via the feet (Fig. 1) is 2 $\times$ 10^{-19} mol/beat released over a period of 20 ms. Values for fraction of cell volume acces-

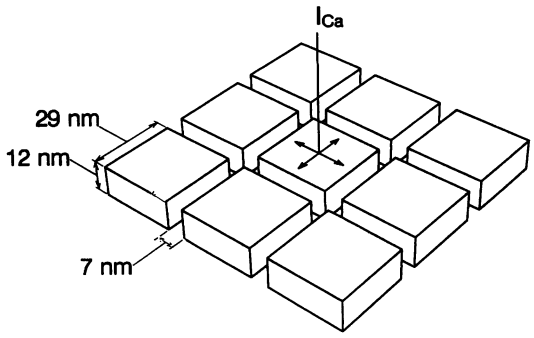

FIGURE 2 Schematic representation of the relation of the Ca "L" channel to the "feet" structures in the cleft. Ratio of number of channels to number of feet is from Wibo et al. (1991). The channel is placed at the center of the 9 "foot" array in the model. The feet and their spacing are to scale and indicate their high density in the cleft space.

sible to Ca vary from 0.4 to a limit of 0.6 (Fabiato, 1983; Sipido and Wier, 1991). Taking an intermediate value of 0.5, the release into the cleft will produce a flux of 8.7 μM/s/liter accessible cell water. This is at the upper end of the range (2.7–9.5 μM/s) reported for SR flux by Sipido and Wier (1991) and would be expected to produce a near-maximum contraction on the basis of Fabiato's (1983) calculations. Because the actual time dependence is not known, we assume a constant release rate (rectangular pulse) of 20 ms duration. We do not include in the model itself any dependence of SR Ca release on the trigger [Ca] in the cleft. Such a dependence must exist, but we leave its inclusion for future work when perhaps more experimental data are available. At present we merely assume a release rate that yields the total Ca release from Fabiato's measurements, which does vary with percentage of maximum force developed.

Mathematical formulation

In a previous paper (Peskoff et al., 1992) we described a nonlinear reaction-diffusion equation governing the diffusion and binding of Ca in the cleft subsequent to its release from the SR, and presented a finite-difference approximation for obtaining numerical solutions to the equation. In the present paper we extend the earlier model so that in addition to the previously considered SR release, diffusion, and binding, we also include Ca leaving the cleft via the Na/Ca exchanger. In addition, we also apply the model to the time period before SR Ca release and consider Ca entering via the Ca channel or by "reverse" Na/Ca exchange and Na entering via the Na channel.

In the model (Fig. 1) [Ca] depends on the radial distance r and time t. The dependence on the distance h perpendicular to the SR and SL surfaces is negligible because the cleft radius/height ratio is large (a/h = 200 nm/12 nm = 16.7) and because of binding. Without binding, the time constant for radial diffusion is $a^2/(5.783D)$ = 0.07 ms (see Peskoff et al., 1992, equation 13). Binding results in an increase of two orders of magnitude in the time constant (Peskoff et al., 1992, or the computations shown in the Results) to a value of ~7 ms. For diffusion in the transverse direction the time constant is $h^2/\pi^2 D = 1.5 \times 10^{-4}$ ms (Crank, 1975), four orders of magnitude faster. Consequently, equilibration in the transverse direction can be considered instantaneous. This reduces the three-dimensional problem to a two-dimensional one. We will consider only radially symmetric distributions of sources, so the problem only depends on one radial distance variable, r, and time, t.

Calcium enters from the SR through approximately 100 feet (Fig. 2), which are believed to be distributed more or less uniformly across the cleft. Consequently, in the model we represent the source of Ca as independent of r. In dealing with the Na/Ca exchangers, of which, in our model, there are also approximately 100 per cleft, we can make the same assumption of a smeared-out Ca source (for "reverse" exchange) or sink (for "forward" exchange) distributed uniformly across the cleft.

The situation is different for the Ca and Na channels, where we expect that at most only one or several channels are conducting at any given time. We will consider the case of a single conducting channel and locate it at the cleft center to maintain the radial symmetry.

The reaction diffusion equation can be written as

$$\frac{\partial c}{\partial t} = \frac{D}{r}\frac{\partial}{\partial r}\left(r\frac{\partial c}{\partial r}\right) + \frac{1}{h}[J_{SR} + J_{bnd} + J_{xch} + J_{chnl}], \quad (1)$$

where, except for the last two terms in square brackets, the equation is essentially the same as appeared in Peskoff et al. (1992). In Eq. 1, r is the radial distance from the center of the cleft, t is time, and $c(r, t)$ is the [Ca] at r and t. $D = 1 \times 10^{-6}$ cm^2 s^{-1} is the diffusion coefficient, and h = 12 nm is the height of the cleft (the SR-to-SL distance). The four terms in square brackets are the flux densities in mol cm^{-2} s^{-1} of Ca entering the cleft from the SR feet, the SL binding sites, the Na/Ca exchanger, and the Ca channel, respectively.

$$J_{SR} = \frac{I_{SR}}{\Pi a^2}, \quad (2)$$

where I_{SR} is the total flux per cleft in mol s^{-1}, and a is the cleft radius. I_{SR} is equal to 1×10^{-17} mol s^{-1} for $0 < t <$ 20 ms and is 0 for $t >$ 20 ms.

The number of moles of Ca bound, c_{bnd} (r, t) mol cm^{-2}, is assumed to be in instantaneous equilibrium with the local [Ca], $c(r, t)$ according to the Michaelis-Menten relationship

$$c_{bnd} = \frac{N_1 c}{K_1 + c} + \frac{N_2 c}{K_2 + c}, \quad (3)$$

where $N_1 = 2 \times 10^{-10}$ and $N_2 = 1.6 \times 10^{-11}$ mol cm^{-2} and are the experimentally measured densities of low- and high-affinity binding sites on the SL (Post and Langer, 1992). K_1 = 1.1 mM and K_2 = 13 μM are the half-saturation values for low- and high-affinity binding, respectively. The flux density into the cleft from the binding sites

is the negative time derivative of c_{bnd}, or differentiating Eq. 3,

$$J_{bnd} = -\frac{\partial c_{bnd}}{\partial t} = -\left[\frac{N_1K_1}{(K_1 + c)^2} + \frac{N_2K_2}{(K_2 + c)^2}\right] \cdot \frac{\partial c}{\partial t}. \quad (4)$$

When the Na/Ca exchanger is operating in the forward direction, i.e., Ca is being moved from the cleft to the extracellular space, we assume that the flux density is related to the [Ca] by

$$J_{xch} = -\frac{Vc}{K_3 + c}, \quad (5)$$

where V is the saturation rate in mol cm^{-2} s^{-1} and $K_3 = 5$ μM is the half-saturation value of c (Hilgemann et al., 1992). V will vary depending on extracellular [Ca], intra- and extracellular [Na], and trans-SL potential according to Matsuoka and Hilgemann (1992), and is stipulated for various conditions in the Results.

To model the time period after SR Ca release (in the Results), Eq. 1 is used with J_{SR}, J_{bnd}, and J_{xch}, given by Eqs. 2, 4, and 5, respectively, and with J_{chnl} set equal to zero. Not including J_{chnl} during this period does not introduce a significant error because the amount of Ca entering through the channel (and through the Na/Ca exchanger operating in reverse) is much less than the SR Ca release that it triggers.

During the time period before SR Ca release (in the Results), Eq. 1 is used with $J_{SR} = 0$ and with $J_{xch} = 0$ when considering the effect of the Ca channel current and with $J_{chnl} = 0$ when considering the effect of "reverse" exchange of Ca.

When the Na/Ca exchanger is operating in reverse, we assume a simple linear relationship between J_{xch} and [Ca],

$$J_{xch} = V \cdot \left(1 - \frac{c}{c_{rev}}\right). \quad (6)$$

Equation 6 will be used only for small excursions of [Ca] (from 0.1 to 0.5 μM) for which the assumption of linearity is acceptable. We use Matsuoka and Hilgemann's (1992, figure 9) data taken at the two values of 0.1 μM and 1.0 μM to determine the values of V and C_{rev}. The two parameters V and C_{rev} are also functions of SL potential and Na concentration. During the initial 10 ms of the action potential, for which we model the effect of reverse exchange, the potential is assumed to be constant at +20 mV. We compute the Na concentration as a function of position and time, but for simplicity, in the reverse exchange computation, we use a single value of [Na] to estimate an upper bound on the effect of reverse exchange on [Ca].

For a single Ca channel located at cleft center, the Ca flux density is

$$J_{chnl} = \begin{cases} I_{chnl}/\Pi b^2, & 0 \le r \le b \\ 0, & b < r \le a, \end{cases} \quad (7)$$

where I_{chnl} is the channel current and b is the radius of the channel mouth.

The Na channel is treated exactly as in Eq. 7, except that I_{chnl} is the Na channel current and the diffusion constant in Eq. 1 is that for Na.

Substituting Eg. 4 in Eq. 1 and solving for $\partial c/\partial t$ yields

$$\frac{\partial c}{\partial t} = \left(1 + \frac{N_1K_1/h}{(K_1 + c)^2} + \frac{N_2K_2/h}{(K_2 + c)^2}\right)^{-1} \cdot \left[\frac{D}{r}\frac{\partial}{\partial r}\left(r\frac{\partial c}{\partial r}\right) + \frac{J_{SR} + J_{xch} + J_{chnl}}{h}\right], \quad (8)$$

where for considering the period before SR release, we take $J_{SR} = 0$ and either $J_{chnl} = 0$ and J_{xch} given by Eq. 6 for reverse exchange, or $J_{xch} = 0$ and J_{chnl} given by Eq. 7 for Ca channel current. For considering the period after SR release, J_{SR} is given by Eq. 2, J_{xch} by Eq. 5, and $J_{chnl} = 0$.

In all cases, the initial condition assumed is that [Ca] at $t = 0$ is at the diastolic value of 0.1 μM throughout the cleft,

$$c(r, 0) = 0.1\ \mu\text{M}, \quad (9)$$

and the boundary condition at the outer limit of the cleft, $r = a$, is

$$c(a, t) = 0.1\ \mu\text{M}. \quad (10)$$

Because [Ca] inside the cleft is found to rise three to four orders of magnitude above the boundary value of Eq. 10, the calculated [Ca] is insensitive to changes in the condition. (We verified this by running the computation with the boundary value increased by an order of magnitude, corresponding to systolic [Ca], with negligible effect.)

The numerical procedure described in Appendix B of Peskoff et al. (1992) was used, with the addition of terms for J_{xch} and J_{chnl}, which were not included there, for obtaining solutions to the initial/boundary value problem of Eqs. 8, 9, and 10. The finite-difference approximation was coded in Fortran and the computation was done on a 486 microcomputer. The reader is referred to the earlier work for details of the numerical recipe. Here we will add only the additional considerations necessary for treating the Ca and Na channel currents.

In the finite-difference computation the continuous spatial variable r ($0 \le r \le 200$ nm) is replaced by the discrete variables $r_n = n\,\Delta r$, with $n = 0, 1, 2, \ldots 40$ and $\Delta r = 5$ nm. Each value r_n for $1 \le n \le 39$ represents an annulus with $r_n - \frac{1}{2}\Delta r \le r \le r_n + \frac{1}{2}\Delta r$. The central point $r_0 = 0$ represents the circle with $0 \le r \le \frac{1}{2}\Delta r = 2.5$ nm. The outermost point, r_{40}, represents the annulus $39.5\,\Delta r \le r \le 40\,\Delta r = 200$ nm.

To maintain radial symmetry, we place the channel at the cleft center. The channel mouth radius b in Eq. 7 is smaller than Δr, and consequently it is below the "resolution" of the numerical computation. Instead of the channel mouth radius, we let $b = \frac{1}{2}\Delta r$ in Eq. 7. Thus we are assuming a current uniformly distributed over a circle of radius 2.5 nm. This is a small enough radius for our purposes, but because it is an order of magnitude larger than the actual Ca channel mouth, in the region between 0 and 2.5 nm, [Ca] will rise to

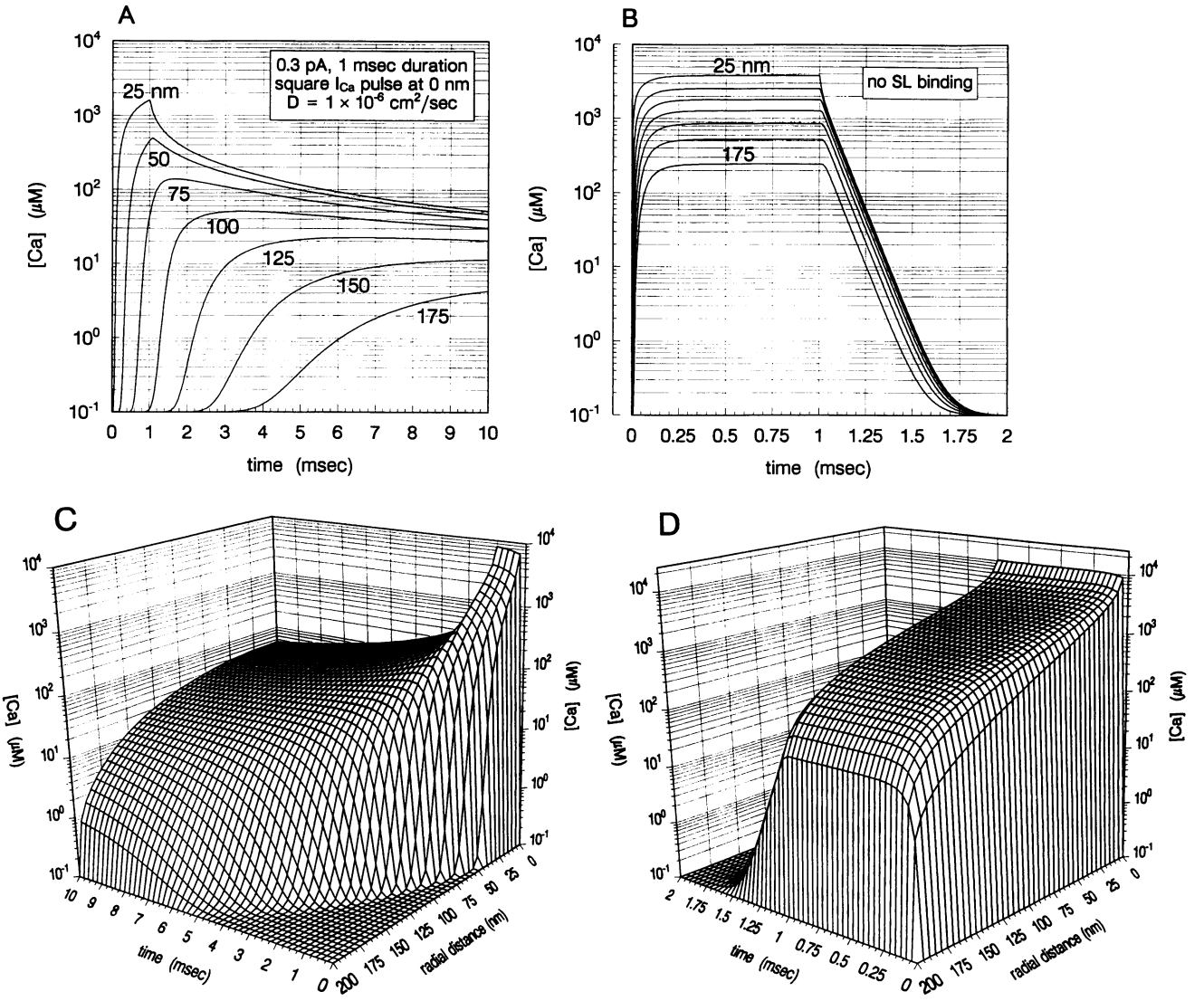

FIGURE 3 (*A*) Ca concentration in the cleft as a function of time after influx via the Ca channel. Influx is in the form of a 1-ms rectangular pulse with a peak current of 0.3 pA from a channel located at $r = 0$ nm. The [Ca] profile at various distances from the cleft center (in 25-nm increments) is shown. (*B*) Ca concentration as in *A*. All parameters are the same, except that the SL binding sites (see Fig. 1) have been removed from the model. Note the expanded time scale and the marked effect on the rate of diffusion of Ca from the cleft space. This emphasizes the major role played by the SL binding sites, particularly the low-affinity (K_d = 1.1 mM) sites, in the determination of Ca concentration and movements in the cleft space. (*C*) Three-dimensional surface plot presentation of computations shown in *A* with [Ca] on the vertical axis, and time and radial distances from cleft center (0 nm) to periphery (200 nm) on the horizontal axes. (*D*) Three-dimensional surface plot presentation of relations as represented in *B* with axes as in *C*. All parameters are as in *C*, except that the SL Ca binding sites have been removed from the model.

higher levels than we calculate. It should be noted also that the computation in effect averages over the dimension (12 nm) between JSR and sarcolemma (Fig. 1). This ignores variations in [Ca] in the transverse direction, which would be large near the channel mouth but not elsewhere. The region near the mouth was considered by Bers and Peskoff (1991, figure 11).

RESULTS

Calcium concentration in the cleft after channel entry

A Ca channel at cleft center is modeled to pass current reaching a maximum 0.3 pA with a rectangular pulse lasting 1 ms. We place the channel at the cleft center $r = 0$ in the center of a 9 "feet" array and expect the results to be qualitatively the same for off-center locations. In the computation, the current I_{Ca} (t) is assumed to enter the cleft at a single central point (Fig. 2).

The [Ca] in the cleft at a point of release 25 nm from cleft center to a radius near the boundary of the cleft (175 nm) over the course of 10 ms is plotted in Fig. 3 *A*. Note that [Ca] rises to >1 mM at 25 nm from the channel at the end of influx and begins to decline at this point relatively rapidly upon closure of the channel. Note the curve designated "50 nm." With an arrangement of channel and feet as depicted in Fig. 2, all nine feet are within a radius of <50 nm from

the channel. Despite a 200-μs delay before [Ca] at 50 nm starts to rise above 100 nm, it reaches 1 μM within 400 μs after influx begins and reaches 10 μM within 500 μs. At 100 nm and beyond [Ca] is still rising while it is declining at points closer to the cleft's center.

The presence of the anionic phospholipid binding sites on the inner sarcolemmal leaflet (Fig. 1) is the single most important factor in the determination of Ca concentration and movement in the cleft space. This is illustrated in Fig. 3 *B*. Note the expanded time scale as compared to Fig. 3 *A*. All parameters are the same as in Fig. 3 *A*, except that the sarcolemmal binding sites have been removed from the model. During the 1-ms period of current flow through the channel, [Ca] rises more rapidly and to higher levels throughout the cleft and establishes a plateau [Ca] during >80% of the time current is flowing. There is also a reduced [Ca] gradient radially across the cleft. The most dramatic difference, however, is the pattern after the channel closes at 1 ms. The [Ca] falls to the 100 nM diastolic level throughout the cleft within 750 μs. Contrast this with the [Ca] decline in Fig. 3 *A*. At 25 nm from cleft center [Ca] is still 50 μM after 10 ms and at the cleft periphery (175 nm) is still rising at the 10th ms. In mid-cleft (100 nm) [Ca] is still 30 μM at 10 ms. The same relations as shown in Fig. 3, *A* and *B*, are shown at 5-nm radial increments in three-dimensional surface plots in Fig. 3, *C* and *D*, respectively. The markedly different patterns show, perhaps even more dramatically, the major effects of the SL binding sites on Ca concentration and movements in the cleft. Again, note the different time scales.

Sodium concentration in the cleft after channel entry

A Na channel placed at the cleft center is modeled to pass a current reaching 2 pA within 500 μs, remaining at this level for 500 μs, and then decreasing linearly with time to 0 pA within 500 μs. The diastolic or resting level of [Na] in the rat ventricular cleft is set at 12.5 mM, which is the level found by Shattock and Bers (1989) in the general cytosol with a microelectrode technique. Note that the diffusion coefficient is twice that assumed for Ca and the binding affinities are 50 times lower. As shown in Fig. 4, at 20 nm from point of release [Na] increases by about 14 mM to reach over 26 mM.

Note, however, the rapid fall after the channel closes and the large gradient across the cleft, even while influx continues for 1.5 ms. This is emphasized in the three-dimensional surface plot of Fig. 4 *B*. The rise of [Na] 40 nm from the channel is about 10 mM. [Na] has returned to resting level throughout the cleft within 750 μs after the channel begins to close. Comparison with Fig. 3, *A* and *C*, emphasizes the striking differences between Ca and Na diffusion within the cleft under the conditions set by the present model (Fig. 1). This difference is caused to a small extent by the difference in diffusion coefficients ($D_{Na} = 2D_{Ca}$) but

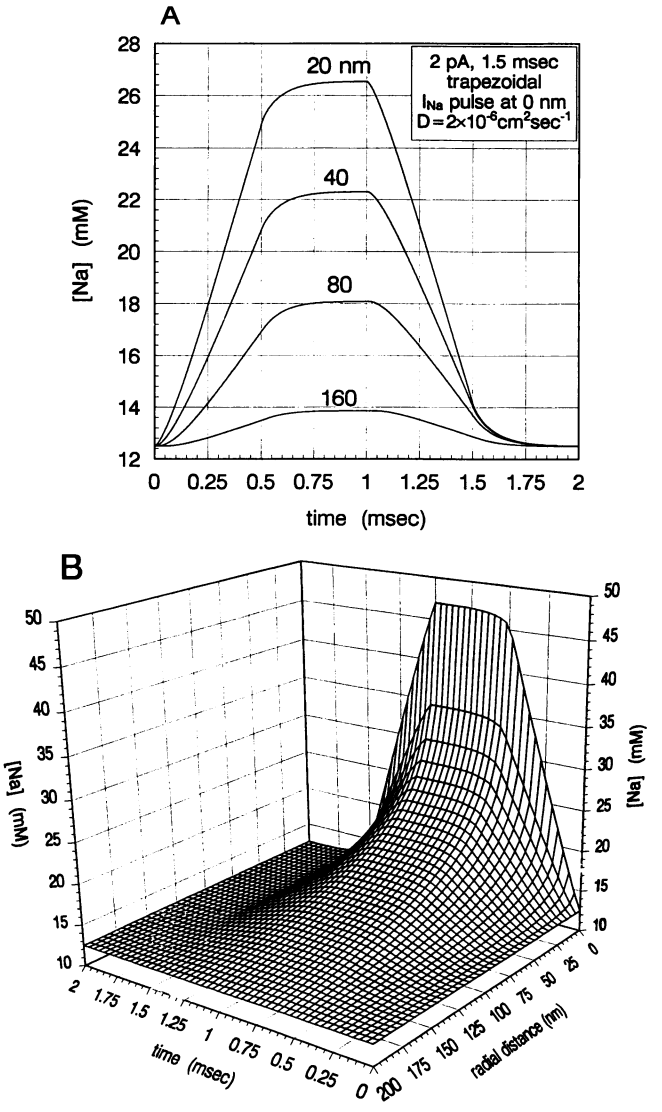

FIGURE 4 (*A*) Sodium concentration in the cleft as a function of time after influx via a Na channel placed at the cleft center ($r = 0$). Influx is in the form of a trapezoidal-shaped pulse with a current peak of 2 pA reached in 500 μs. Compare with the [Ca] profile in Fig. 3 *A*. The resting [Na] is taken from the results of Shattock and Bers (1989). (*B*) Three-dimensional surface plot presentation of computation shown in *A* with [Na] on the vertical axis and time and radial distance on the horizontal axes.

mostly by the 50-fold decrease in Na binding at the SL as compared to Ca binding.

Calcium concentration as a result of "reverse" Na/Ca exchange

As shown by Matsuoka and Hilgemann (1992) at $[Na]_i$ levels of >10 mM the Na/Ca exchanger current becomes outward (net movement of Ca inward) at membrane depolarizations more positive than 0 mV. Therefore it is to be expected, as originally proposed by Leblanc and Hume (1990), that with depolarization there would be a net movement of Ca into the cell via the Na/Ca exchangers in the

sarcolemma. We have used the experimental data of Matsuoka and Hilgemman (1992) in our computation to estimate the exchanger current at the cleft as the rat cell depolarizes to +20 mV and remains at this level for 10 ms (Schouten and ter Keurs, 1985). We find that [Ca] in the cleft increases from 0.1 μM to about 0.5 μM during this time, as shown in Fig. 5. The changing [Ca] that is computed is used to determine the instantaneous Na/Ca exchanger current over the 10-ms period (the outward current is assumed to decrease linearly with [Ca] as $[Ca]_i$ rises from 0.1 to 1 μM, fit to the Matsuoka and Hilgemann data). At 800 exchanges/μm^2 (Fig. 1), the 0.13 μm^2 cleft will contain 100 exchangers, which, according to the results of Matsuoka and Hilgemann, will be operating at 12% exchanger's V_{max} (outward, 5000 cycles/s) as depolarization to +20 mV occurs with $[Ca]_i$ 0.1 μM and with no net current at +20 mV with the $[Ca]_i$ 1.0 μM. An average $[Na]_i$ of 16 mM is assumed over the 10-ms period, and this exaggerates the effect on reverse Na/Ca exchange because, as seen in Fig. 4 *A*, [Na] returns to 12.5 μM within 700 μs after influx ceases. Because there are 100 exchangers operating (in contrast to the Ca and Na channels, where we expect one conducting per cleft) we assume the exchange current to be distributed uniformly over the cleft area rather than occurring at a single location.

Given the input of the exchangers distributed throughout the cleft and the slow Ca diffusion, there is little difference in [Ca] from the center outward to 150 nm. Because, under the conditions of the model, there is the same number of exchangers as "feet," >50% of the feet will "see" the same Ca concentration at about the same time. The outer ring of feet will see a lesser concentration as Ca diffuses out to the cytosol—thus note the 175-nm line in Fig. 5. As seen, a concentration of exchangers at the diadic cleft that generates an initial outward current (net Ca influx) at 12% maximum is capable of raising [Ca] at over 50% of the cleft surface to 0.5 μM within 8 to 10 ms. In terms of whole cell current this would require about 0.3 nA in this period.

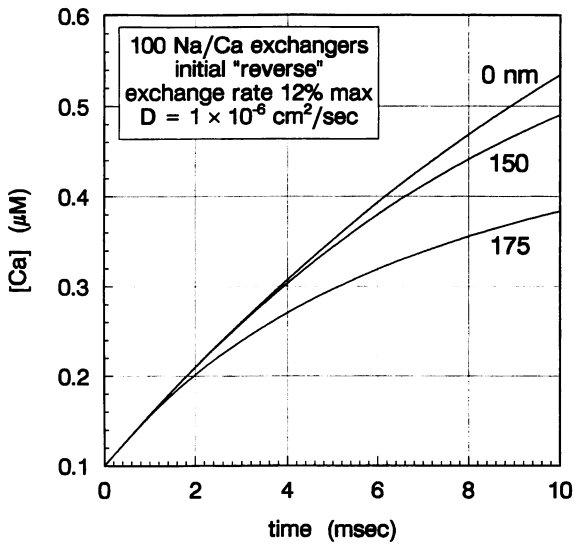

FIGURE 5 Ca concentration in the cleft as a function of time as determined by "reverse" Na/Ca exchange. One hundred Na/Ca exchangers are distributed homogeneously over the cleft SL membrane, and V_m is clamped at +20 mV. The changing [Ca] as shown is used to determine the instantaneous Na/Ca exchanger current over the 10-ms period. The outward current is assumed to decrease linearly with [Ca] as it rises from 0.1 to 1 μM and is calculated to fit the results from Matsuoka and Hilgemann (1992). Compare with the [Ca] profile as generated by influx via the Ca channel in Fig. 3 *A*.

Calcium concentration in the cleft after JSR release

Regardless of whether Ca release through the feet is triggered by Ca through the "L" channels or via "reversed Na/Ca exchange," release from the SR is the next step in the excitation-contraction coupling process and, given the location of the feet, the release obviously occurs into the cleft space (Fig. 1). The resultant course of Ca concentration in the cleft is illustrated in Fig. 6 *A*. The amount of Ca released is sufficient to produce near-maximum force development. This translates to 2×10^{-19} mol into a single cleft with each contraction. The latency period between excitation and contraction indicates that this release occurs over about 20 ms. It should be reemphasized that the model is for the rat ventricle beating at a rate of 300/min, which means a single contraction cycle is 200 ms in length. Of this 200 ms about half is occupied by the rat's triangularly shaped action potential (Schouten and ter Keurs, 1985), with a peak depolarization of +20 mV and a resting potential of about −85 mV. Computation of the mean transmembrane potential for the 200-ms cycle gives a value of −60 mV. Using the data from Matsuoka and Hilgemann (1992) we can calculate the velocity of the exchanger at −60 mV when saturated with Ca. This velocity is very close to 30% of the 5000 cycles/s V_{max} of the exchanger (Hilgemann et al., 1991) or 1500 cycles/s. This value is, then, the operative V_{max} at −60 mV, and the velocity will then change according to the Michaelis-Menten relation: $V = (1500/s)/(1 + K_d/[Ca])$, where $K_d = 5$ μM (Hilgemann et al., 1992) and $[Ca]_i$ is the Ca concentration at each radial position and each instant during the cycle.

Assuming that the release is uniformly distributed throughout the cleft space, Fig. 6 *A* shows the concentration from cleft center (0 nm) to the periphery (175 nm) as Ca is released over 20 ms and then diffuses out of the cleft to the cytoplasm and is transported out of the cell by the Na/Ca exchangers. It is striking that [Ca] reaches 600 μM at cleft center and >100 μM at cleft periphery at end release. Concentration then falls rapidly to reach the diastolic level of 100 nM throughout the space at about 170 ms. Note that at longer times, the model predicts continued expulsion of Ca such that [Ca] dips below 100 μM. This will not continue because with resting potential in the −90 mV range net outward movement of Ca will cease and [Ca] will stabilize. At the end of the contraction cycle (beyond 140

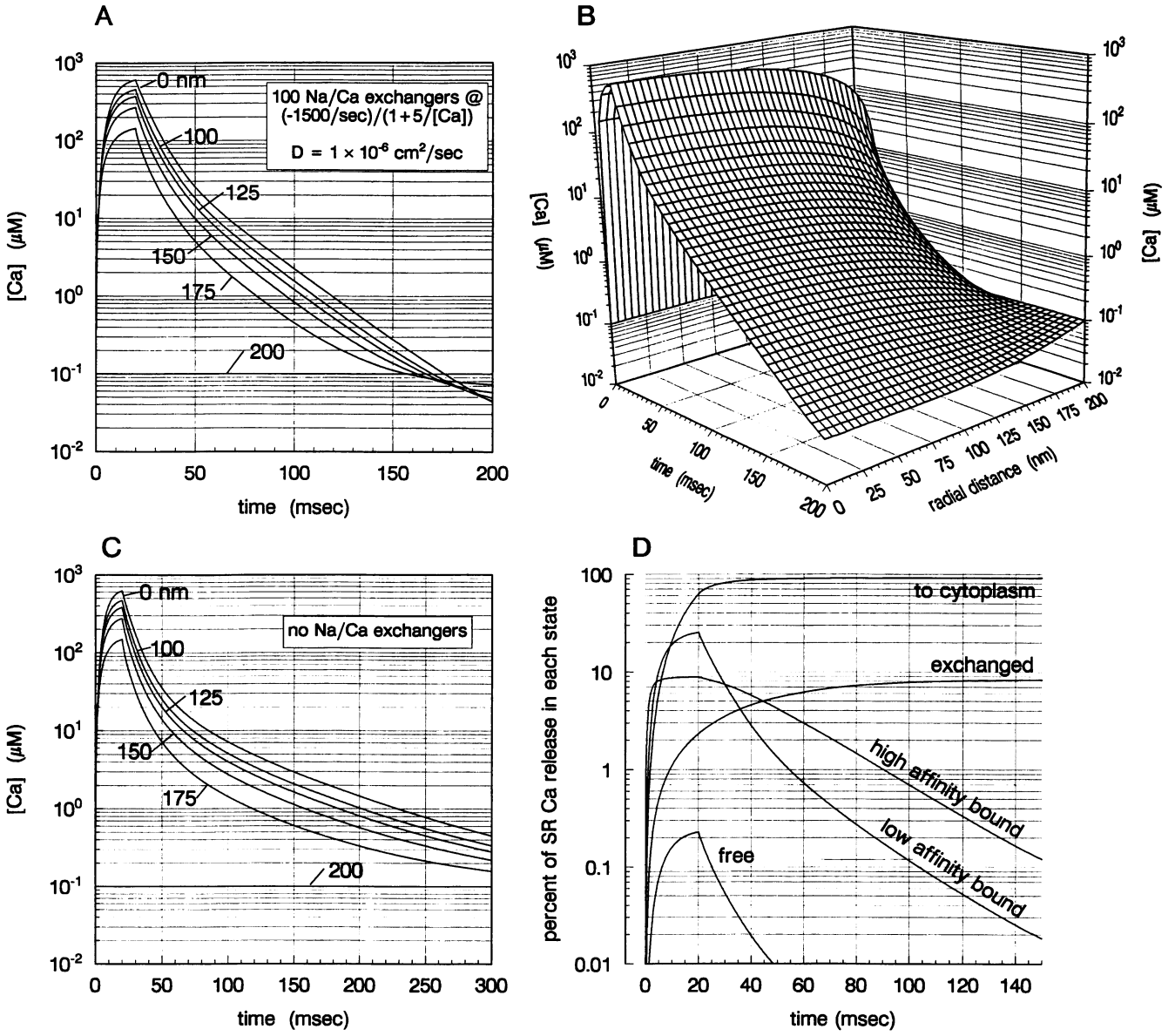

FIGURE 6 (*A*) Ca concentration in the cleft as a function of time during and after uniform release throughout the cleft space from the JSR feet. Release takes 20 ms and then ceases. During the period plotted V_m is assumed to be −60 mV (see text), which sets the velocity of the exchangers at 30% V_{max} according to Matsuoka and Hilgemann (1992). The velocity then changes with instantaneous [Ca] according to Michaelis-Menten kinetics. K_d (Ca) is taken as 5 μM (Hilgemann et al., 1992) with a Na/Ca exchanger density of 100 distributed homogeneously throughout the cleft SL membrane. Concentration at cleft center (0 nm) and at various points to the periphery (200 nm) is indicated. Note that [Ca] has returned to resting level (10^{-1} μM) throughout the cleft 150 ms after release ceases. (*B*) Three-dimensional surface plot presentation of computation shown in (*A*), with [Ca] on the vertical axis and time and radial distance from cleft center (0 nm) to periphery (200 nm) on the horizontal axes. (*C*) All parameters as in *A*, except that all Na/Ca exchangers have been removed from the model such that all Ca released diffuses to the cytoplasm and none exits the cell via the exchangers. Compare with *A* and note that [Ca] is still at 1 μM, or 10 × higher, throughout most of the cleft 150 ms after release ceases. This emphasizes the importance of exchangers localized to the cleft space in clearing Ca before the next release occurs. (*D*) Percentage of total Ca ions free, bound, exchanged, and diffused to cytoplasm as a function of time after JSR release. At any instant after release ceases (at the 20th ms) addition of all fractions totals 100% of the amount released. Note that at completion of release two-thirds of the Ca destined for the cytoplasm has left the cleft, but that three-quarters of the Ca destined to exit via the Na/Ca exchangers is still in the cleft space. Of this latter fraction 99% is bound to the low- and high-affinity sites and <1% is free in the space. All parameters as in *A*.

ms) the amount of Ca extruded is trivial (see Fig. 6 *D*), because current is very small at these low levels of [Ca]. The relation shown in Fig. 6 *A* is shown in the three-dimensional surface plot in Fig. 6 *B*.

Release of half the amount of Ca (1×10^{-19} mol) modeled in Fig. 6, *A* and *B*, will produce about 30% maximum force (Fabiato, 1983). Ca reaches >200 μM at cleft center and >60 μM at cleft periphery at end release and

then decreases at essentially the same rate as shown in Fig. 6 *A*.

Fig. 6 *C* depicts results for the same conditions as Fig. 6 *A*, except that all Na/Ca exchangers have been removed from the cleft, so that all Ca released from the feet diffuses to the cytoplasm and none exits the cell via the exchangers. Note that [Ca] is still >1 μM at 150 ms, whereas it is an order of magnitude lower with the exchangers operative (Fig. 6 *A*). It is still at >1 μM at the center of the cleft when the next stimulation is due at 200 ms, and this would make it difficult, if not impossible, to trigger Ca release for the next contraction. We assume here that there is no resequestration of Ca from the cleft space by pumps in the cisternal SR, although some studies (Holmberg and Williams, 1990) indicate some cisternal pumping capacity. This would, of course, reduce $[Ca]_i$ more rapidly.

In Fig. 6 *D* we have integrated over the cleft volume to get the total number of Ca ions free, bound, exchanged, and diffused to the cytoplasm, as a function of time after JSR release. The amounts have been normalized with respect to the total SR release, so that at any instant after release is completed ($t > 20$ ms) addition of all fractions adds to 100% of the amount released. Note that with the amount of released Ca necessary to activate near-maximum force slightly more than 90% escapes from the cleft to the cytoplasm and less than 10% leaves the cell via the exchangers. At the end of release from the JSR (20 ms) about 0.2% of all Ca released is free in the cleft, about 25% is bound to the low-affinity phospholipid sites on the sarcolemma, and about 9% is bound to the high-affinity sarcolemmal sites. By 50 ms (30 ms after termination of release) virtually all (98%) of the Ca that is destined for the cytoplasm has left the cleft, whereas the remainder of Ca to be transported out of the cell via Na/Ca exchange is derived from the low- and high-affinity binding sites (Fig. 6 *D*).

Fraction of SR released Ca leaving the cell via Na/Ca exchange

It is to be expected that as the amount of Ca released into the cleft varies, so should the amount transported out via the exchanger. Fig. 7 shows this relationship at a variety of K_d(Ca) values for the exchanger and for variable amounts of SR release per kilogram wet weight of whole heart. The release from 0 up to 100 μmol/kg wet wt heart covers the range from 0 to full activation of the myofilaments (Fabiato, 1983). For example, release of 30 μmol Ca is predicted at $K_d = 5$ μM (*middle curve*) to deliver 80% or 24 μmol to the cytoplasm and remove 20% or 6 μmol from the cell via the exchanger. Such release to the cytoplasm will barely activate the myofilaments (Fabiato, 1983). Release of 100 μmol Ca will deliver 92 μmol to the cytoplasm for full myofilament activation, and 8 μmol will exit the cell via the exchanger. The curves with the various K_d values tend to merge as the amount released increases because the exchangers become saturated, even at the higher K_d values.

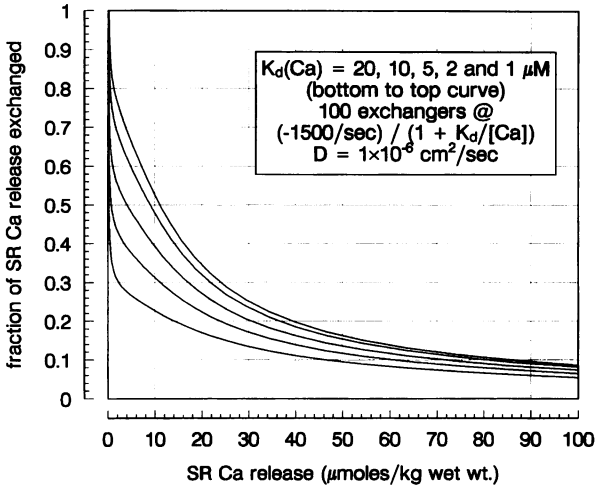

FIGURE 7 Fraction of released Ca leaving the cell via Na/Ca exchange as a function of the amount released. The curves represent different K_d (Ca) for the exchangers (20, 10, 5, 2, 1 μM, *bottom to top curve*). Cleft parameters other than K_d (Ca) are as for Fig. 6 *A*. Note that at high levels of release the fraction expelled changes little as release increases. Thus transport of Ca out of the cell becomes directly proportional to the amount released. Release is per kilogram wet weight of ventricle.

The effect of concentration of binding sites in the cleft on the rate of Ca efflux via Na/Ca exchange is shown in Fig. 8. For the calculation the JSR release was as indicated in Fig. 1 and stops at the 20-ms point. Because [Ca] in the cleft rises well above 100 μM during release whether or not binding sites are present, efflux rate is not affected during this 20-ms period. Note, however, the marked effect of

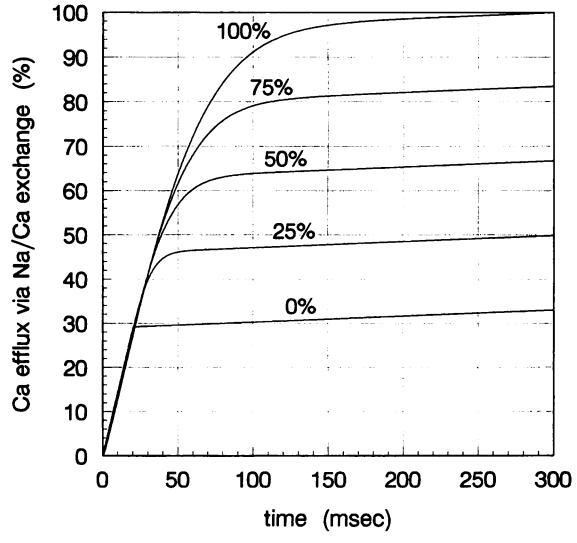

FIGURE 8 The effect on Ca efflux, via Na/Ca exchange, of removal of inner-leaflet SL anionic binding sites. Ca is released via the feet into the cleft space for 20 ms. With a full complement of anionic sites (100% curve, same as "exchanged" curve in Fig. 6 *D*) Ca efflux via the exchangers is ~98% complete by 200 ms. As anionic sites are removed in a graded fashion Ca efflux via the exchangers falls progressively. With no binding (0% curve) only ~32% of total required efflux is achieved by 200 ms.

removal of binding sites after release ceases. At the extreme, under the conditions of the model, extrapolation of the "0%" curve indicates that >3 s would be required for the exchangers to exchange the 8 μmol (Fig. 7) required for the maintenance of a steady-state level of Ca in the cell.

DISCUSSION

The signal for Ca-induced Ca release

It has been assumed since the elegant work of Fabiato and Fabiato (1975) that SR Ca release was triggered by entry of Ca through "L" channels. In 1990, however, Leblanc and Hume (1990) proposed an alternative mechanism by which Ca entry via the Na/Ca exchanger could serve as the trigger. Much evidence has accumulated to support such a mechanism (Levi et al., 1994; Lipp and Niggli, 1994; Nuss and Houser, 1992), but recent results indicate that Ca transported through Ca channels is many times more effective in gating SR release (Sham et al., 1995; Cannell et al., 1994) than is Na/Ca exchange.

The Ca concentration in the cleft space as affected by the two mechanisms is compared in Figs. 3 and 5 under the conditions of the present model. It is obvious that Ca entering via the channel will increase [Ca] to 1 μM within a distance of 50 nm from the channel in less than 500 μs (Fig. 3, *A* and *C*). Therefore, all nine feet within the domain of the Ca channel (Fig. 2) will "see" a minimum 1 μM concentration at a maximum time of 500 μs. According to Fabiato (1985, p. 272, figure 12) this concentration increase within this time will release an amount of Ca sufficient to activate >50% maximum force.

Now compare the [Ca] change induced in the cleft space due to influx via the Na/Ca exchanger (Fig. 5). At 1 ms [Na] reaches a maximum of 26 mM at 20 nm from the opening of the channel but is 18 mM 80 nm away (Fig. 4). Unless the cleft has a preferential concentration of Na channels it is unlikely that a single cleft of 0.13 μm^2 area would have more than one channel (Fozzard et al., 1985) and extremely unlikely that it would open again during the depolarization, which is "clamped" at +20 mV for the 10-ms period shown in Fig. 5. Under these conditions of voltage and $[Na]_i$ the Na/Ca exchangers will be operating in a net Ca influx mode at 12% of its maximum rate (Matsuoka and Hilgemann, 1992) during the first millisecond, by which time, according to Fig. 5, it will have increased [Ca] by only 60 nM throughout most of the cleft space. This will trigger little, if any, Ca release (Fabiato, 1985). If the +20 mV depolarization is maintained [Ca] will reach 0.5 μM in 10 ms, which would produce about 20% activation of contractile force. However, if a Ca channel opens into a cleft, within microseconds of depolarization the local $[Ca]_i$ increase (Fig. 3 *A*) will rapidly take the exchangers in the direction of Ca extrusion and obviate the onset of any "reverse" Na/Ca exchange. It is clear, under the present conditions modeled for the rat ventricle, that Ca channel influx is a much more efficient mechanism of stimulating Ca release. This is in agreement with the recent findings of Sham et al. (1995) for rat ventricle. This is not to say that in the absence of Ca current or under conditions where it may be delayed or reduced that "reversed" Na/Ca exchange is not capable of providing the trigger. For example, Levi et al. (1994) depolarized to strongly positive potentials where Ca current declined but phasic contraction increased. Such a finding would be expected by voltages in the +30 to +60 range because the curves in Fig. 5 would be elevated as net Ca influx via the exchangers is enhanced. A reduction in $[Na]_O$ would have a similar effect, and such was found by Levi et al. when 0[Na] was perfused 50 ms before and 50 ms after depolarization.

Although Ca entry via the channel is fully capable of providing a strong trigger stimulus over a domain of nine receptors (Fig. 2) according to the present model, this stimulus could be augmented by a chain reaction in which the cluster of SR channels are mutually coupled by their own Ca release, as proposed by Stern (1992). Although such a mechanism would possibly be redundant for triggering from a channel, its locally regenerative release could significantly amplify a relatively weak stimulus based on "reversed" Na/Ca exchange (Fig. 5).

Calcium in the cleft after JSR release

The next step in the cell's excitation-contraction coupling process is release from the JSR into the cleft space via the "feet" (Fig. 1). In the present model we release the amount necessary to achieve full myofilament activation according to Fabiato (1983). This is released over a period of 20 ms. The cleft [Ca] versus time is shown in Fig. 6 *A*, with 100 exchangers turning over at 1500 cycles/s when fully saturated with Ca at a transmembrane potential of −60 mV (see Results). [Ca] rises to >100 μM even at the periphery of the cleft (175 nm) and then declines rapidly when release ceases. As Ca diffuses from the cleft to the cytoplasm and is transported out via the Na/Ca exchangers the radial diversity declines, and at 170 ms (150 ms after release ceases) all Ca within the cleft is at the 100 nM diastolic level. The functioning of the cleft as a subcellular Ca compartment is emphasized by the three-dimensional plot (Fig. 6 *B*).

The importance of the operation of Na/Ca exchange within the cleft is illustrated in Fig. 6 *C*. This shows the [Ca] versus time after the same release as in Fig. 6 *A* but without Na/Ca exchange, i.e., Ca leaves the cleft only by diffusion to the cytoplasm. Note that [Ca] is >1 μM at 150 ms, whereas it is an order of magnitude lower with the exchangers operative. It is still >700 nM at the cleft center at the time the next stimulation is due at 200 ms. This comparison, i.e., the cleft space with and without the concentration of Na/Ca exchangers, is strong evidence in support of the model. The cleft containing the "feet" is clearly the space into which the JSR releases its Ca. If exchangers are not localized to the space and operative under the conditions

proposed by the current model, the released Ca will not be cleared rapidly enough to restore the Ca release channels to the state in which they can be induced again to release Ca upon the next stimulation (Fabiato, 1985).

The Ca distribution among the elements of the cleft as shown in Fig. 6 *D* is of interest. It emphasizes the fact that shortly after the release from JSR is completed at 20 ms, 72% of the Ca to be removed from the cleft by the exchangers remains, and of this remainder >99% is bound to the low- and high-affinity sites and <1% is free. It is, then, the bound Ca on the sarcolemma that is responsible for maintenance of cleft [Ca] at levels sufficient to stimulate the exchangers with K_d(Ca) of 5 μM, so that Ca efflux from the cell can be completed before the next cycle and the steady-state cellular Ca level can be maintained. If the binding sites were not present, [Ca] in the cleft would plummet to 100 nM within 1 ms (Fig. 3 *B*) and Ca efflux from the cleft space via Na/Ca exchange would be greatly reduced. This relation is explored further in the next section.

We have assumed in this model that all of the Na/Ca exchange takes place in the cleft regions. The other extreme is that all exchange takes place over the entire sarcolemmal surface, including the "T" tubes, with no specialized cleft structure to facilitate Na/Ca exchange. With this distribution, and the same functional characteristics for the exchangers as presented, it would require ~1 s to expel the amount of Ca entering via the Ca channels. Therefore, at a beat rate of >60/min the exchangers would fail to remove all of the Ca entering the cell with each beat and a progressive increase of intracellular Ca would occur. It is fair to assume that there is a "noncleft" exchange in the cell, but it is not sufficient to maintain steady-state Ca levels, except at basal contraction frequency.

One might also assume a smaller radius for the cleft. If the cleft radius were half that modeled (a = 0.1 μm, Fig. 1), the Ca efflux from the cleft would decrease by >50%. Such a reduction would make maintenance of steady-state $[Ca]_i$ difficult.

The exchanger flux:cytosolic flux ratio

Under the conditions of the model exchange flux is predicted to respond to the amount of Ca released into the cleft space. This is clearly shown in Fig. 7, with the exchangers operating as in Fig. 6 *A*. Using the middle curve of Fig. 7 (K_d (Ca) = 5 μM) it is seen that with SR release of 10 μmol/kg heart, below the level for myofilament activation, 40% of the release or 4 μmol will exit the cell. A tenfold increase in release (100 μmol) is associated with about 8% leaving via the exchangers or 8 μmol. Thus, over the range from 0 to maximum activation (Fabiato, 1983), Ca efflux via the exchangers doubles. Eight micromoles per kilogram wet weight translates into approximately 1.6×10^{-16} mol/cell. We have previously measured the total integrated Ca current over a range from 15% to nearly 100% of force activation in the rat ventricular cell (Wang et al., 1993). At 60% activation the integrated current indicates that 1.7×10^{-16} mol enter the cells through the Ca channels. This value is close to that calculated for efflux via Na/Ca exchange from the clefts and is consistent with the requirement that the exchanger efflux match the channel influx so that steady-state levels of Ca are maintained in the cell. The 8 μmol Ca/kg wet weight leaving the cell via the exchanger represents 8% of the total Ca release of 100 μmol (see above and Fig. 7). This is in agreement with Bassani et al. (1994), who found that during a twitch 7% of the Ca involved in a twitch was transported by Na/Ca exchange in isolated rat ventricular myocytes.

Fig. 8 illustrates the importance of the inner-leaflet binding sites for the efficient operation of the cleft exchangers. If no binding sites were present (0% curve in Fig. 8) it would require >3 s to remove 8 μmol Ca via the exchangers. Therefore, steady-state intracellular [Ca] could not be maintained if the heart rate was >20/min and most Ca efflux took place at the clefts.

CONCLUSIONS

Under the physiological conditions set for rat ventricle with the present model it is predicted that triggering of JSR Ca release will occur by Ca entry through "L"-type Ca channels. Channel influx will produce a [Ca] of >1 μM over a domain of nine "feet" in 500 μs. "Reverse" Na/Ca exchange, on the other hand, requires 10 ms to raise [Ca] to 0.5 μM. This is capable of triggering release, but to a level that would produce <20% activation of contractile force (Fabiato, 1985). Given the same level of SR Ca loading, the channel influx would trigger release capable of producing >50% activation over a much reduced time as compared to "reverse" Na/Ca exchange. It should be noted, however, that Ca channel opening is a stochastic process (Rose et al., 1992) and may be delayed for many milliseconds after depolarization at a particular cleft. In this case, "reverse" Na/Ca exchange would be the process likely to trigger Ca release.

It is generally accepted that Ca from the JSR is released from the "feet" and, therefore, into the cleft space. This introduces two important constraints, at least for rat ventricle beating at 300/min or more: 1) Ca must be cleared from the region where the feet are located rapidly enough to reduce [Ca] to resting levels before the next stimulation or triggering will not occur. This clearly requires that there be a concentration of Na/Ca exchangers in the cleft (Fig. 6 *A* compared to Fig. 6 *C*). 2) For the exchangers within the cleft to operate at a level sufficient to clear the Ca, the [Ca] in the cleft must be at levels near their K_d(Ca) for tens of milliseconds after JSR release has ceased (Fig. 6 *A* and 8). This requires the presence of the sarcolemmal binding sites (Fig. 1), especially those of low affinity (Fig. 6 *D*). If these sites are not present (Fig. 3 *B*), Ca within the cleft will diffuse to the cytoplasm at a rate that will cause [Ca] to reach resting levels (100

nM) in <1 ms. This would eliminate effective operation of the Na/Ca exchangers in the region (Fig. 8).

Finally, in an attempt to be as concise as possible we have selected various specific examples for application of the cleft model. Results will certainly vary as other species, fluxes, currents, and conditions are applied. There is an almost infinite number of combinations. We expect, however, that the present model will serve as a foundation for the calculation of ion movements in restricted spaces bordered by binding sites, wherever they may exist.

REFERENCES

Bassani, J. W. M., R. A. Bassani, and D. M. Bers. 1994. Relaxation in rabbit and rat cardiac cells: species-dependent differences in cellular mechanisms. *J. Physiol. (Lond.).* 476:279–293.

Bassingthwaighte, J. B., and H. Reuter. 1972. Calcium movements and excitation-contraction coupling in cardiac cells. *In* Electrical Phenomena in the Heart. DeMello, W. C., editors. Academic Press, London. 353–395.

Berlin, J. R., and M. Konishi. 1993. Ca^{2+} transients in cardiac myocytes measured with high and low affinity indicators. *Biophys. J.* 65: 1632–1647.

Bers, D. M., and A. Peskoff, 1991. Diffusion around a cardiac calcium channel and the role of surface bound calcium. *Biophys. J.* 59:703–721.

Bockris, J. O'M., and A. K. N. Reddy. 1970. Modern Electrochemistry, Vol. 1. Plenum Press, New York.

Böhle, T., and K. Benndorf. 1995. Multimodal action of single Na^+ channels in myocardial mouse cells. *Biophys. J.* 68:121–130.

Cannell, M. B., H. Cheng, and W. J. Lederer. 1994. Spatial non-uniformities in $[Ca^{2+}]_i$ during excitation-contraction coupling in cardiac myocytes. *Biophys. J.* 67:1942–1956.

Carmeliet, E. 1992. A fuzzy subsarcolemmal space for Na^+ in cardiac cells? *Cardiovasc. Res.* 26:433–442.

Crank, J. 1975. The Mathematics of Diffusion, 2nd ed. Clarendon Press, Oxford.

Fabiato, A. 1983. Calcium induced release of calcium from cardiac sarcoplasmic reticulum. *Am. J. Physiol.* 245:C1–C14.

Fabiato, A. 1985. Time and calcium dependence of activation and inactivation of calcium-induced release of calcium from the sarcoplasmic reticulum of a skinned canine cardiac Purkinje cell. *J. Gen. Physiol.* 85:247–289.

Fabiato, A., and F. Fabiato. 1975. Contractions induced by a calcium-triggered release of calcium from the sarcoplasmic reticulum of single skinned cardiac cells. *J. Physiol. (Lond.).* 249:469–495.

Fozzard, H. A., C. T. January, and J. C. Makielski. 1985. New studies of the excitation sodium currents in heart muscle. *Circ. Res.* 56:475–485.

Frank, J. S. 1990. Ultrastructure of the unfixed myocardial sarcolemma and cell surface. *In* Calcium and the Heart. G. A. Langer, editor. Raven Press, New York. 1–25.

Frank, J. S., G. Mottino, D. Reid, R. S. Molday, and K. D. Philipson. 1992. Distribution of the Na^+-Ca^{2+} exchange protein in mammalian cardiac myocytes: an immuno-fluorescence and immunocolloidal gold-labeling study. *J. Cell Biol.* 117:337–345.

Hilgemann, D. W., A. Collins, and S. Matsuoka. 1992. Steady-state and dynamic properties of cardiac sodium-calcium exchange: secondary modulation by cytoplasmic calcium and ATP. *J. Gen. Physiol.* 100: 933–961.

Hilgemann, D. W., D. A. Nicoll, and K. D. Philipson. 1991. Charge movement during Na^+ translocation by native and cloned cardiac Na^+/Ca^{2+} exchanger. *Nature.* 352:715–718.

Hodgkin, A. L., and R. D. Keynes. 1957. Movement of labeled calcium in squid giant axons. *J. Physiol. (Lond.).* 138:253–281.

Holmberg, S. R. M., and A. J. Williams. 1990. The cardiac sarcoplasmic reticulum calcium release channel: modulation of ryanodine binding and single channel activity. *Biochim. Biophys. Acta.* 1022:187–193.

Ikemoto, N., B. Antoniu, J-J. Kang, L. G. Mészáros, and M. Ronjat. 1991. Intravesicular calcium transients during calcium release from sarcoplasmic reticulum. *Biochemistry.* 30:5230–5237.

Inui, M., A. Saito, and S. Fleischer. 1987. Isolation of the ryanodine receptor form cardiac sarcoplasmic reticulum and identity with the feet structures. *J. Biol. Chem.* 262:15637–15642.

Jorgenson, A. O., A. Shen, W. Arnold, P. S. McPherson, and K. P. Campbell. 1993. The Ca^{2+} release channel/ryanodine receptor is localized in junctional, and corbular sarcoplasmic reticulum in cardiac muscle. *J. Cell Biol.* 120:969–980.

Kargacin, G. J. 1994. Calcium signaling in restricted diffusion spaces. *Biophys. J.* 67:262–272.

Kushmerick, M. J., and R. J. Podolsky, 1969. Ionic mobility in muscle cells. *Science.* 166:1297–1298.

Langer, G. A., S. Y. Wang, and T. L. Rich. 1995. Localization of the Na/Ca exchange-dependent Ca compartment in cultured neonatal rat heart cells. *Am. J. Physiol.* 268:C119–C126.

Leblanc, N., and J. R. Hume. 1990. Sodium current-induced release of calcium from cardiac sarcoplasmic reticulum. *Science.* 248:372–376.

Lederer, W. J., E. Niggli, and R. W. Hadley. 1990. Sodium-calcium exchange in excitable cells: fuzzy space. *Science.* 248:283.

Legato, M. J. 1979. Cellular mechanisms of normal growth in the mammalian heart. II. A quantitative and qualitative comparison between right and left ventricular myocytes in the dog from birth to five months of age. *Circ. Res.* 44:263–279.

Levi, A. J., K. W. Spitzer, O. Kohmoto, and J. H. B. Bridge. 1994. Depolarization-induced Ca entry via Na-Ca exchange triggers SR release in guinea pig cardiac myocytes. *Am. J. Physiol.* 266: H1422–H1433.

Lipp, P., and E. Niggli. 1994. Sodium current-induced calcium signals in isolated guinea pig ventricular myocytes. *J. Physiol. (Lond.).* 474: 439–446.

Matsuoka, S., and D. Hilgemann. 1992. Steady-state and dynamic properties of cardiac sodium-calcium exchange. Ion and voltage dependencies of the transport cycle. *J. Gen. Physiol.* 100:963–1001.

Moore, E. D. W., E. F. Etter, K. D. Philipson, W. A. Carrington, K. E. Fogarty, L. M. Lifshitz, and F. S. Fay. 1993. Coupling of the Na^+-Ca^{2+} exchanger, Na^+/K^+ pump and sarcoplasmic reticulum in smooth muscle. *Nature.* 365:657–660.

Nasi, E., and D. Tillotson. 1985. The rate of diffusion of Ca^{2+} and Ba^{2+} on a nerve cell body. *Biophys. J.* 47:735–738.

Niggli, E., and P. Lipp. 1993. Subcellular restricted spaces: significance for cell signaling and excitation-contraction coupling. *J. Muscle Res. Cell Motil.* 14:288–291.

Nowycky, M. C., and M. J. Pinter. 1993. Time courses of calcium and calcium bound buffers following calcium influx in a model cell. *Biophys. J.* 64:77–91.

Nuss, H. B., and S. R. Houser. 1992. Sodium-calcium exchange-mediated contraction in feline ventricular myocytes. *Am. J. Physiol.* 263: H1161–H1169.

Ohki, S., and R. Kurland. 1981. Surface potential of phosphatidylserine monolayers. II. Divalent and monovalent ion binding. *Biochim. Biophys. Acta.* 645:179–176.

Page, E. 1978. Quantitative ultrastructural analysis in cardiac membrane physiology. *Am. J. Physiol.* 4:C147–C158.

Peskoff, A., J. A. Post, and G. A. Langer. 1992. Sarcolemma calcium binding sites in heart. II. Mathematical model for diffusion of calcium released from the sarcoplasmic reticulum into the diadic region. *J. Membr. Biol.* 129:59–69.

Post, J. A., J. H. Kuwata, and G. A. Langer. 1993. A discrete Na^+/Ca^{2+} exchange dependent, Ca^{2+} compartment in cultured neonatal rat heart cells. Characteristics, localization and possible physiological function. *Cell Calcium.* 14:61–71.

Post, J. A., and G. A. Langer. 1992. Sarcolemmal calcium binding site in heart. I. Molecular origin in "gas-dissected" sarcolemma. *J. Membr. Biol.* 129:48–57.

Post, J. A., G. A. Langer, J. A. F. Opden Kamp, and A. J. Verkleij. 1988. Phospholipid asymmetry in cardiac sarcolemma. Analysis of intact cells and "gas-dissected" membranes. *Biochim. Biophys. Acta.* 943:256–266.

Radermacher, M., V. Rao, R. Grassuci, J. Frank, A. P. Timerman, S. Fleischer, and T. Wagenknecht. 1994. Cryo-electron microscopy and three-dimensional reconstruction of the calcium release channel/ryanodine receptor from skeletal muscle. *J. Cell Biol.* 127: 411–423.

Rose, W. C., C. W. Balke, W. G. Wier, and E. Marban. 1992. Macroscopic and unitary properties of physiological ion flux through L-type Ca^{2+} channels in guinea pig heart cells. *J. Physiol.* 456:267–284.

Sakakibara, Y., T. Furukawa, D. H. Singer, H. Jia, C. L. Backer, C. E. Artenzen, and J. A. Wasserstrom. 1993. Sodium current in isolated human ventricular myocytes. *Am. J. Physiol.* 265:H1301–H1309.

Schouten, V. J. A., and H. ter Keurs. 1985. The slow repolarization phase of the action potential in rat heart. *J. Physiol. (Lond.).* 360:13–35.

Sham, J. S. K., L. Cleeman, and M. Marad. 1995. Functional coupling of Ca^{2+} channels and ryanodine receptors in cardiac myocytes. *Proc. Natl. Acad. Sci. USA.* 92:121–125.

Shattock, M. J., and D. Bers. 1989. Rat vs. rabbit ventricle: Ca flux and intracellular Na assessed by ion-selective microelectrodes. *Am. J. Physiol.* 256:C813–C822.

Sipido, K. R., and W. G. Wier. 1991. Flux of Ca^{2+} across the sarcoplasmic reticulum of guinea-pig cardiac cells during excitation-contraction coupling. *J. Physiol. (Lond.).* 435:605–630.

Stern, M. D. 1992. Theory of excitation-contraction coupling in cardiac muscle. *Biophys. J.* 63:497–517.

Stewart, J. M., and E. Page. 1978. Improved stereological techniques for studying myocardial cell growth: application to external sarcolemma, T system and intercalated disks of rabbit and rat hearts. *J. Ultrastruct. Res.* 65:119–134.

Wang, J. H. 1953. Tracer diffusion in liquid. IV. Self-diffusion of calcium ion and chloride ion in aqueous calcium chloride solutions. *J. Am. Chem. Soc.* 75:1769–1770.

Wang, S. Y., L. Winka, and G. A. Langer. 1993. Role of calcium current and sarcoplasmic reticulum calcium release in control of myocardial contraction in rat and rabbit myocytes. *J. Mol. Cell Cardiol.* 25:1339–1347.

Wibo, M., Bravo, G., and T. Godfraind. 1991. Postnatal maturation of excitation-contraction coupling in rat ventricle in relation to the subcellular localization and surface density of 1,4-hydropyridine and ryanodine receptors. *Circ. Res.* 68:662–673.